Hindawi
International Journal of Photoenergy
Volume 2020, Article ID 8870194, 8 pages
https://doi.org/10.1155/2020/8870194

Research Article

Shift the Photocatalytic Activity of P25 TiO_2 Nanoparticles toward the Visible Region upon Surface Modification with Organic Hybrid of Phosphotungstate

Mehdi Taghdiri[1,2] **and Shahrban Dadari Doolabi**[1]

[1]*Department of Chemistry, Payame Noor University, 19395-3697 Tehran, Iran*
[2]*Research Center of Environmental Chemistry, Payame Noor University, Ardakan, Yazd, Iran*

Correspondence should be addressed to Mehdi Taghdiri; mehditaghdiri@yahoo.com

Received 2 August 2020; Revised 30 September 2020; Accepted 12 October 2020; Published 2 November 2020

Academic Editor: Hao Li

In this study, a visible-light-driven P25 TiO_2 was prepared upon surface modification with a colored organic hybrid of phosphotungstic acid that makes titanium dioxide suitable for photocatalytic degradation of organic pollutants under visible and sunlight irradiation. Visible shifting of the photocatalytic activity of surface-modified TiO_2 was examined by studying the decolorization of methylene blue (MB) and rhodamine B (RhB). The results show that colored TiO_2 is, unlike bare TiO_2, a good photocatalyst in the degradation of dyes under visible and sunlight irradiation. Surface-modified Al_2O_3 and reduced graphene oxide (RGO) with organic hybrid of phosphotungstate failed to degrade RhB under sunlight irradiation, which prove the role of TiO_2 in the photochemical process.

1. Introduction

The major limitation of P25 TiO_2 as a photocatalyst is its poor efficiency in the visible region of the solar spectrum due to wide band gap of 3.2 eV, which typically requires exposure of ultraviolet (UV) light for photocatalytic reactions. Hence, the photocatalytic application of TiO_2 at an industrial scale has been limited because only 4-5% of the solar spectrum corresponds to UV photons. Therefore, strong efforts have been devoted to activating the TiO_2 toward the visible and solar light for application purposes [1, 2]. One of the approaches for attainment of this issue is dye sensitization, i.e., the adsorption of dyes especially phthalocyanines on the TiO_2 surface [3–8]. One other is modification with polyoxometalates (POMs), but pure POMs cannot shift the photocatalytic activity of pure P25 TiO_2 toward the visible region, and it is necessary to join them to valuable metallic or nonmetallic moieties [9–13]. In this work and in the following of our previous works [14, 15], we have utilized the combination of dye sensitization and POMs, i.e., the adsorbed MB on phosphotungstate-hexamethylenetetramine hybrid (PTA-HMT-MB) as sensitizer. To our knowledge, the coating of P25 TiO_2 with a colored organic hybrid of POMs has not been reported yet. The hybridization and immobilization onto P25 TiO_2 resolve high solubility and poor recyclability of POMs and facilitate separation because coated TiO_2 is not suspended in the solution.

2. Experimental

2.1. Chemicals and Reagents. The P25 TiO_2 was from Plasma-Chem GmbH (Berlin, Germany) with the nominal 21 ± 10 nm particle size, and the phosphotungstic acid hydrate ($H_3PW_{12}O_{40}{\cdot}xH_2O$, total impurities < 0.06%) was from Fluka. The hexamethylenetetramine (HMT) ($C_6H_{12}N_4$, 99.5%) was from Sina Chemical Industries Co. (Shiraz, Iran). Activated alumina (Al_2O_3) and reduced graphene oxide (RGO) were

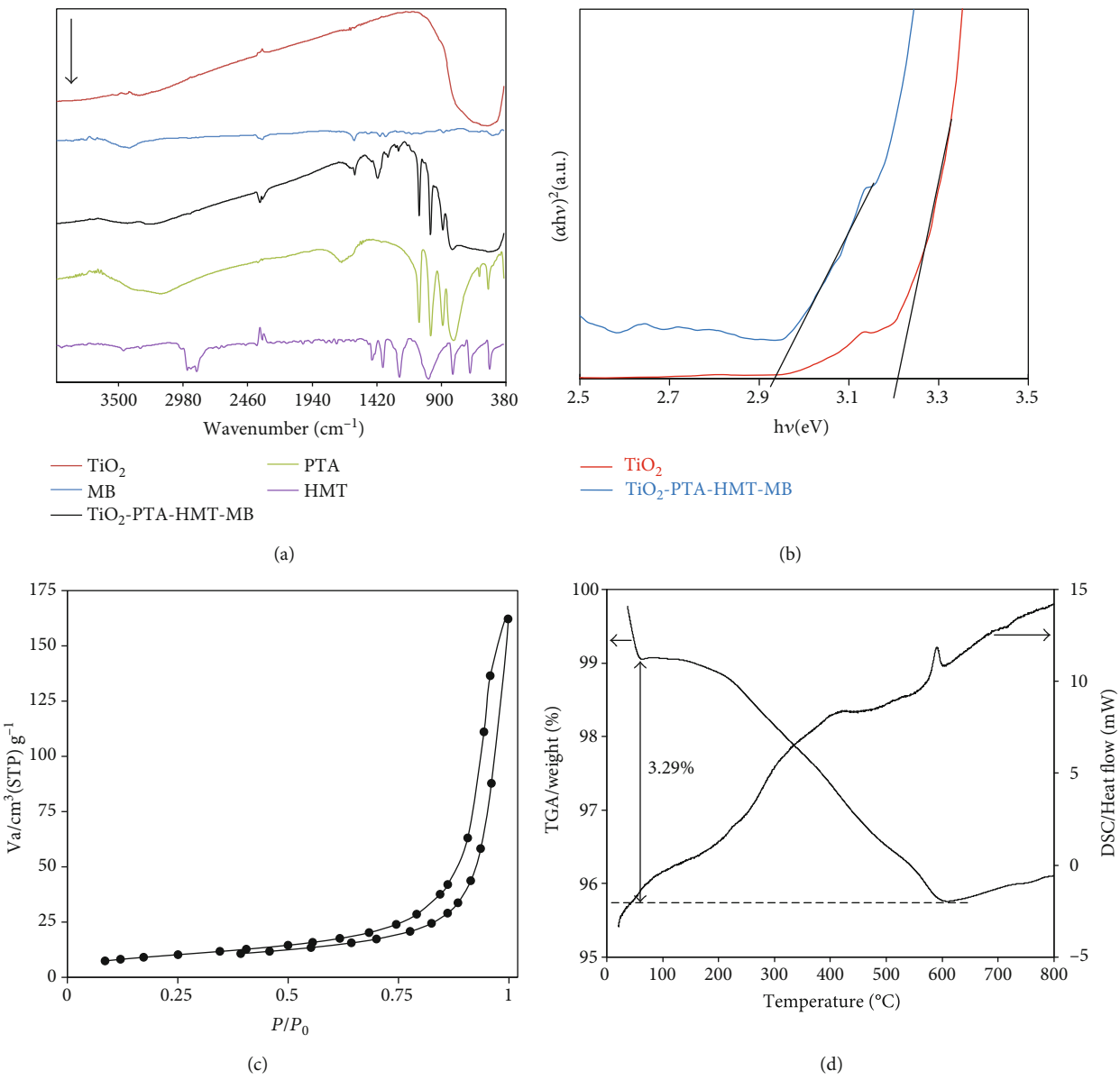

Figure 1: (a) FTIR spectra, (b) Tauc's plots of TiO_2 and TiO_2-PTA-HMT-MB for determining the band gap energy from variation of $(\alpha h\nu)^2$ with photon energy ($h\nu$), (c) N_2 adsorption-desorption isotherm, and (d) TGA and DSC curves of TiO_2-PTA-HMT-MB.

consigned by Ardakan Industrial Ceramics Co. (Ardakan, Iran) and Nanostructured Coatings Institute (Yazd, Iran), respectively. Other reagents were purchased from commercial sources and used without further purification.

2.2. Apparatus. The stirring of solutions was performed using a Labinco magnetic stirrer model L-81. A Metrohm type 691 pH meter was used for pH measurements. UV-Vis absorption spectra were obtained using a GBC model Cintra 6 or Shimadzu 1601PC spectrophotometer. The IR spectra were conducted on a Shimadzu 8400s FTIR spectrometer. Diffuse reflectance spectra (DRS) were recorded on an Avantes spectrometer (AvaSpec-2048-TEC), using $BaSO_4$ as a standard. The surface area and pore volume of the composite were measured and calculated by the BET method from nitrogen adsorption-desorption isotherms at 77 K with a surface area and pore size analyzer (BELSORP-mini II, Bel, Japan). The thermogravimetric analysis (TGA) and differential scanning calorimetry (DSC) were performed on a Rheometric Scientific STA 1500 thermal analyzer under the atmosphere of air. Scanning electron microscopy (SEM) and transmission

Table 1: Textural parameters of the P25 TiO_2 and TiO_2-PTA-HMT-MB composite.

Sample	Surface area (m^2/g)	Mean pore diameter (nm)	Total pore volume (cm^3g^{-1})
P25 TiO_2	56.191	18.062	0.2537
TiO_2-PTA-HMT-MB	28.372	31.795	0.2255

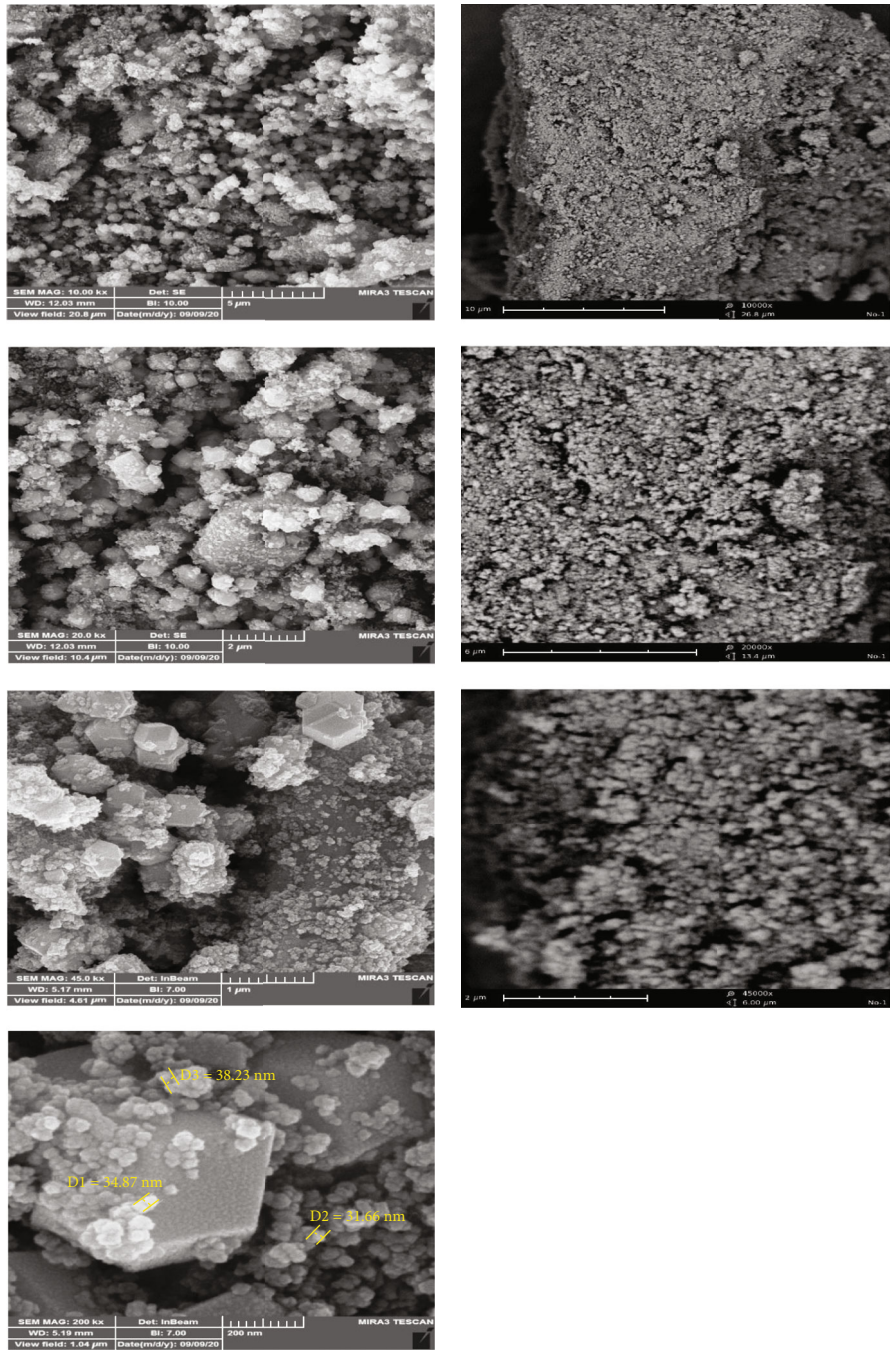

(a) (b)

Figure 2: SEM images of TiO_2-PTA-HMT-MB (a) and TiO_2 (b) at magnifications of 10000, 20000, 45000, and 200000 (from top to down).

electron microscopy (TEM) for TiO_2-PTA-HMT-MB were performed using FESEM TESCAN MIRA3 and TEM Philips EM 208S, respectively.

2.3. Preparation of Composites. The TiO_2-PTA-HMT-MB composite was prepared in two steps. In the first step, the PTA-HMT was prepared according to our previous works [15, 16]. 10 mL hexamethylenetetramine aqueous solution (1.0% *w*/*w*) was mixed with a 10 mL phosphotungstic acid aqueous solution (7.5% *w*/*w*). The immediate result was a milky suspension, which was magnetically stirred at 500 rpm for 3 h at an ambient temperature. Then, the white precipitate was filtered, washed with distilled water, and dried at 100°C. In the second step, the modified P25 TiO_2 nanopowder, i.e., TiO_2-PTA-HMT-MB, was obtained by adding 0.195 g PTA-HMT to 50 mL MB solution (134 mg L^{-1}), and the pH of the mixture reached 2.5. Then, 0.195 g P25 TiO_2 was added to it, and the solution was stirred for 6 h. At the end, the precipitate was filtered and dried in an oven for 3 h, at 100°C. The Al_2O_3-PTA-HMT-MB and

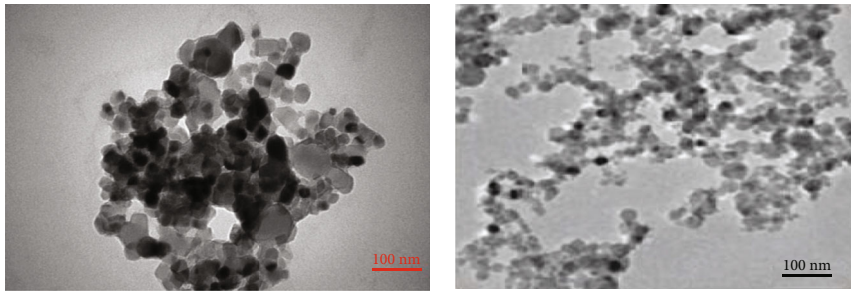

(a) (b)

Figure 3: TEM image of TiO_2-PTA-HMT-MB (a) and P25 TiO_2 (b).

RGO-PTA-HMT-MB composites were prepared similar to the above manner.

2.4. Evaluation of the Photocatalytic Activity. Solar photocatalytic experiments were performed similar to our previous works [14, 15]. 100 mL RhB (15 mg L^{-1}) and a specific amount of the photocatalyst were transferred to a beaker, capped by cellophane, and exposed to sunlight in September 2017 between 11 am and 3 pm at the Payame Noor University, Ardakan, Yazd, Iran (GPS coordinates: 32°29′N, 53°59′E). The experiments were conducted without stirring during solar irradiation. The visible light experiments were carried out using a metal halide lamp (500 W, Philips). 15 mL MB solutions (30 mg L^{-1}) and a predetermined amount of the photocatalyst were transferred to a 200 mL water-cooled cylindrical Pyrex vessel reactor. The distance between the reactor and the light source was 10 cm. The radiation intensity is about 900 W/m^2 [17]. The reaction was started by switching on the light source after adding the composite to the dye solutions. The reactor was placed on a magnetic stirrer and stirred continuously. Temperature of the reactor was maintained at 27°C by considering a cooling chamber around the reactor and circulating water in it. During two processes, at given time intervals, 4 mL of suspension was withdrawn, and the composite was removed and then analyzed by a UV-Vis spectrophotometer. The C/C_0 values were obtained through the maximum absorption in the whole absorption spectrum in order to plot C/C_0 vs. time curves.

3. Results and Discussion

3.1. Characterizations. The IR spectrum of TiO_2-PTA-HMT-MB exhibits the characteristic bands of the HMT and MB organic moieties and of TiO_2 and PTA inorganic moieties (Figure 1(a)). The band positioned at 555 cm^{-1} refers to the symmetric stretching of TiO_2. The strong absorption peaks at 1100-750 cm^{-1} show the presence of $PW_{12}O_{40}^{3-}$ anions with the α-Keggin structure. The 887 cm^{-1} band is related to the W-O_b-W stretching mode of PTA while the 987 cm^{-1} band corresponds to its W-O_d scissoring mode. The peak about 1250 cm^{-1} can be attributed to the vibration of the CH_2 of HMT [18], and the 1597 cm^{-1} corresponds to the vibration of the aromatic ring of MB [19]. The band gaps of TiO_2 and TiO_2-PTA-HMT-MB were determined from the diffuse reflectance spectra using Tauc's plots (Figure 1(b)). It is clear that there are differences in the band gap values of TiO_2 and modified TiO_2. The band gap of TiO_2-PTA-HMT-MB (2.94 eV) has been shifted to the visible region (422 nm) in comparison with the band gap of TiO_2 (3.2 eV, 388 nm). To determine the specific surface area, total pore volume and mean pore diameter of the TiO_2-PTA-HMT-MB, BET analysis method, and N_2 adsorption-desorption measurement (Figure 1(c)) were used. The measured specific surface area of the composite was 28.372 m^2/g, which is lower than that of TiO_2 (56.191 m^2/g). Indeed, the pores are loaded by the PTA-HMT-MB hybrid. The mean pore diameter and total pore volume were 31.795 nm and 0.2255 cm^3g^{-1}, respectively. Textural parameters of the P25 TiO_2 and TiO_2-PTA-HMT-MB hybrid are compared in Table 1. According to the IUPAC classification, the mentioned mean pore diameter belongs to the mesopore groups [20]. The TG and DSC curves of the TiO_2-PTA-HMT-MB composite are shown in Figure 1(d). The exothermic peak at 593°C is related to the decomposition of phosphotungstate to WO_3 and P_2O_5. The weight loss of 3.29% is ascribed to the loss of the organic

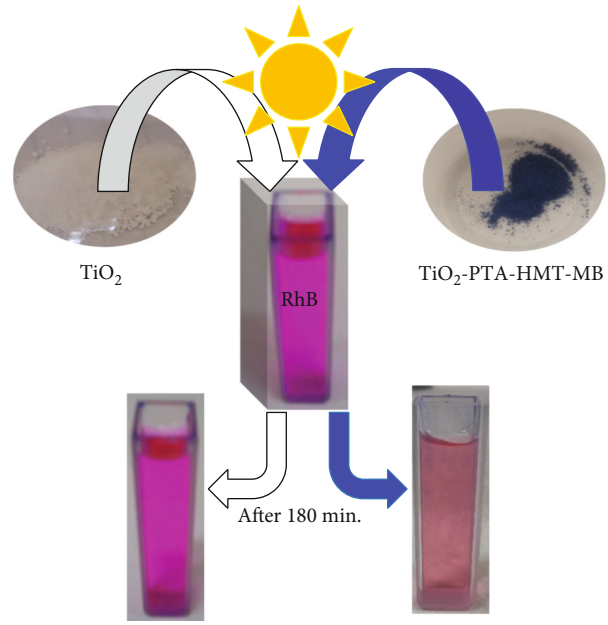

Scheme 1: Schematic illustration of the solar photocatalytic experiment for RhB.

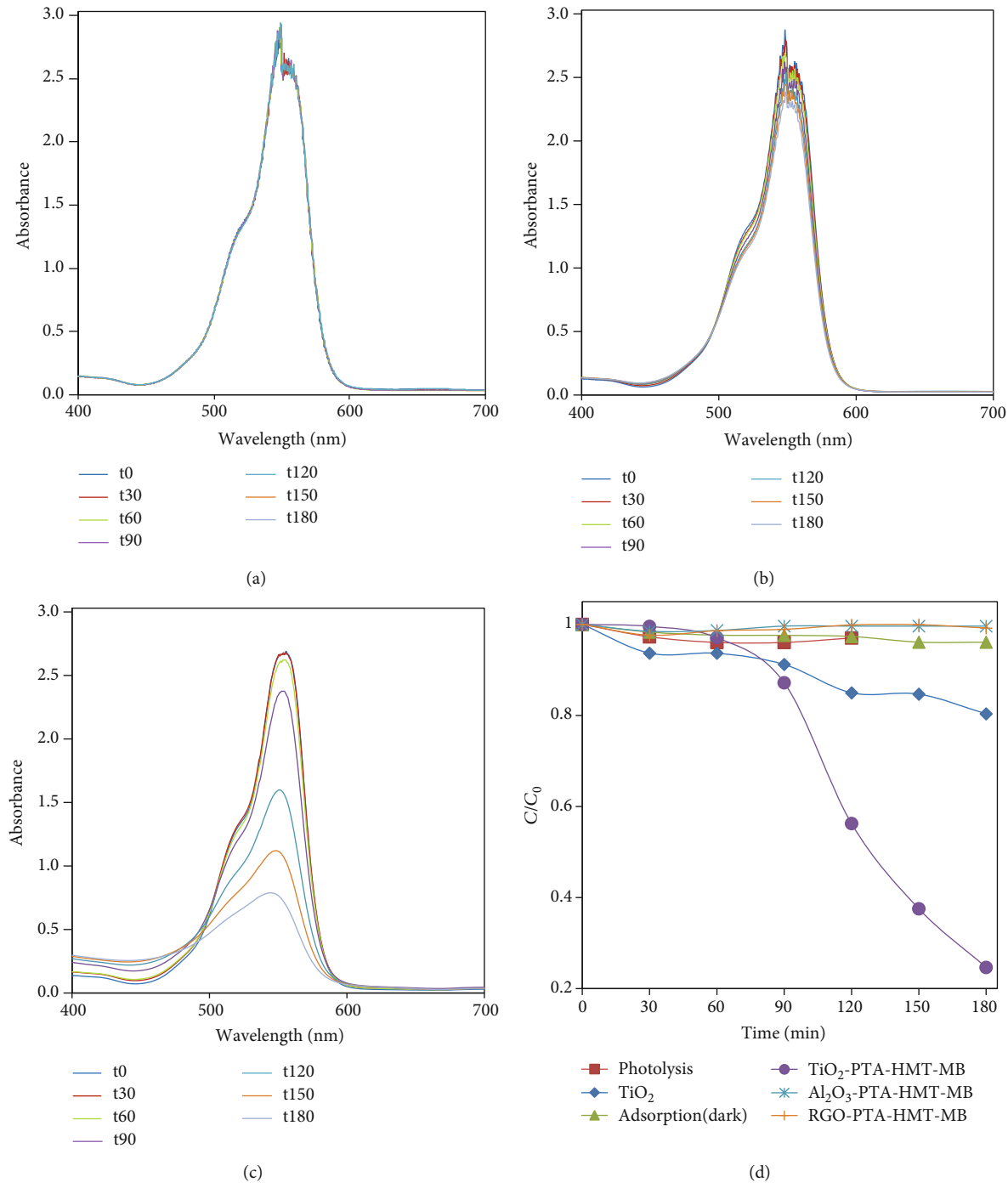

Figure 4: UV-Vis absorption spectra of RhB (15 mg/L, 100 mL, pH = 9.0) during the photodegradation under sunlight without photocatalyst (photolysis) (a), in the presence of TiO_2 (0.15 g/L) (b), in the presence of TiO_2-PTA-HMT-MB (0.1 g/L) (c), and C/C_0 vs. time curves (d).

moieties of the composite, i.e., HMT-MB. Figure 2 shows the SEM images of TiO_2-PTA-HMT-MB and TiO_2 nanoparticles. Comparison of these images displays that uniform distribution and neat morphology of TiO_2 nanoparticles are not observed in TiO_2-PTA-HMT-MB nanoparticles. The TEM images in Figure 3 show that modified TiO_2 nanoparticles agglomerated to larger particles with an irregular shape than P25 TiO_2. The sizes of TiO_2-PTA-HMT-MB nanoparticles were estimated from the TEM image in the range of 30–80 nm which are in agreement with the sizes obtained from the SEM image (Figure 2).

3.2. Photocatalytic Degradation of RhB. The composite was applied for photodecomposition of RhB under sunlight irradiation. Schematic illustration of the photocatalytic experiment is shown in Scheme 1. UV-Vis absorption

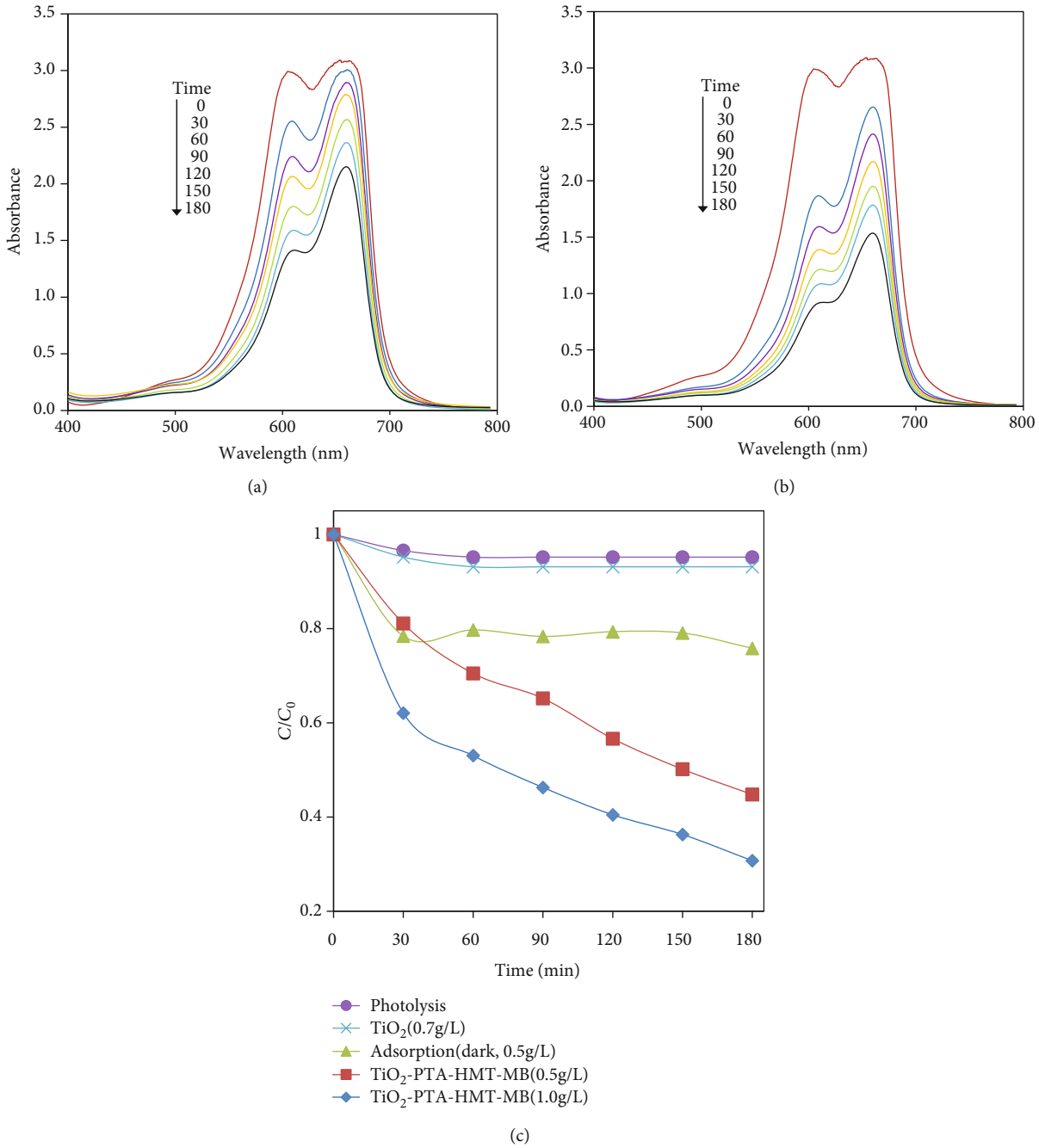

Figure 5: UV-Vis absorption spectra of MB (30 mg/L, pH = without adjustment = 5.7) during the photodegradation under visible light in the presence of TiO_2-PTA-HMT-MB (0.5 g/L) (a), (1.0 g/L) (b), and C/C_0 vs. time curves (c).

spectra of RhB (15 mg/L, 100 mL, pH = 9.0) during the photodegradation under sunlight without photocatalyst (photolysis), in the presence of TiO_2 and modified TiO_2, are shown in Figures 4(a)–4(c). TiO_2-PTA-HMT-MB cannot adsorb RhB because RhB ($pK_a = 3.1$) is in neutral form at pH 9.0 (Figure 4(d)). The photodegradation of RhB is negligible due to photolysis and in the presence of TiO_2 (0.15 g/L) (Figure 4(d)). However, it becomes noticeable in the presence of TiO_2-PTA-HMT-MB (0.1 g/L) that is an indicative shift in the photocatalytic activity of P25 TiO_2 nanoparticles toward the visible region upon surface modification with phosphotungstate hybrid. The composites of Al_2O_3-PTA-HMT-MB and RGO-PTA-HMT-MB failed to degrade RhB under sunlight irradiation (Figure 4(d)), which prove the role of TiO_2 in the photochemical process. Indeed, an excited surface-adsorbed hybrid (PTA-HMT-MB) injects a charge into the conduction band of TiO_2, and then reactive radicals are produced and degrade RhB.

3.3. Photocatalytic Degradation of MB. The composite was then tested as a catalyst for the photocatalytic degradation

Table 2: Comparison of photodegradation of dyes by using TiO_2-PTA-HMT-MB and reported P25 TiO_2-POMs.

Catalysts	Light	C_{dye} (mg/L)	Catalyst dosage (g/L)	Time (min)	Decolorization (%)	Ref.
$TiW_{11}Ti/TiO_2$	UV	Brilliant dye X-3B (40)	0.59	20	97.4	[22]
$HP_{62}W_{18}O_{62}/TiO_2/\beta$-zeolite	UV	MO (16)	1.4	180	65[a]	[23]
Fe-PTA/P25	Simulated sunlight	MB (20)	50 mg + 50 mmol H_2O_2[b]	12	47[a]	[24]
P25-PEI-$P_2Mo_{15}V_3$	Simulated sunlight	MB (40)	0.25	115	75[a]	[25]
P25 TiO_2-PTA-HMT-MB	Sunlight	RhB (15)	0.1	180	75.3	This work
P25 TiO_2-PTA-HMT-MB	Vis.	MB (30)	1.0	180	69.3	This work

[a]Value was estimated from original figure of the reference; [b]volume of solution is unknown. Note: PEI: polyethyleneimine; MO: methyl orange.

of MB under visible light. While the P25 TiO_2 (0.7 g/L) shows very low photocatalytic activity toward MB degradation, the TiO_2-PTA-HMT-MB is very active (Figure 5). The photodegradation without photocatalyst (photolysis) and the removal of MB due to adsorption on the composite were evaluated in order to indicate the performance of the TiO_2-PTA-HMT-MB photocatalyst (Figure 5(c)).

3.4. Comparison with Other P25 TiO_2-POM Composites. Until now, many studies have been conducted in order to modify titanium dioxide [1, 21], but the majority have used the sol-gel method not P25 TiO_2. The photocatalytic efficiency of the TiO_2-PTA-HMT-MB composite is compared with other P25 TiO_2-POM composites in Table 2. It should be noted that the light sources are visible light and sunlight in this work while these are UV light and simulated sunlight in other works. As it is seen, the combination of P25 TiO_2 with lone POMs such as $TiW_{11}Ti$ [22] and $HP_{62}W_{18}O_{62}$ [23] does not shift the photocatalytic activity to visible light. However, this purpose has been achieved by the incorporation of a third component together with POMs such as Fe [24], polyethyleneimine [25], and HMT-MB (this work). The findings show that the advantage of the present photocatalyst is the shift of the photocatalytic activity toward the visible region, and hence, it shows the photocatalytic behavior under a visible light source (metal halide lamp) in addition to sunlight.

4. Conclusion

In summary, P25 TiO_2 was coated with PTA-HMT-MB hybrid. The TiO_2-PTA-HMT-MB composite indicated a narrower band gap than P25 TiO_2. The photocatalytic performance was evaluated by the photodegradation of RhB and MB under solar and visible light, respectively. The decolorization of these dyes with pure P25 TiO_2 in the solar/visible light is negligible while the POM hybrid coating causes decolorization with TiO_2-PTA-HMT-MB to be remarkable. This work presents the incorporation of an organic hybrid of phosphotungstate as an effective strategy for exploration of shifting the photocatalytic activity of P25 TiO_2 toward the visible region, thereby facilitating the solar light driven photocatalysis.

Data Availability

The readers can access the supporting data through contact with the corresponding author.

Conflicts of Interest

The authors declare that there is no conflict of interest regarding the publication of this paper.

Acknowledgments

This work was supported by Payame Noor University. The authors express their appreciation for support of this study.

References

[1] M. Humayun, F. Raziq, A. Khan, and W. Luo, "Modification strategies of TiO_2 for potential applications in photocatalysis: a critical review," *Green Chemistry Letters and Reviews*, vol. 11, no. 2, pp. 86–102, 2018.

[2] Y. Liu, J.-F. Wan, C.-T. Liu, and Y.-B. Li, "Fabrication of magnetic $Fe_3O_4/C/TiO_2$ composites with nanotube structure and enhanced photocatalytic activity," *Materials Science and Technology*, vol. 32, no. 8, pp. 786–793, 2016.

[3] D. Chatterjee and A. Mahata, "Visible light induced photodegradation of organic pollutants on dye adsorbed TiO_2 surface," *Journal of Photochemistry and Photobiology A: Chemistry*, vol. 153, no. 1-3, pp. 199–204, 2002.

[4] S. Xu, W. Lu, S. Chen et al., "Colored TiO_2 composites embedded on fabrics as photocatalysts: Decontamination of formaldehyde and deactivation of bacteria in water and air," *Chemical Engineering Journal*, vol. 375, article 121949, 2019.

[5] V. Iliev, "Phthalocyanine-modified titania—catalyst for photooxidation of phenols by irradiation with visible light," *Journal of Photochemistry and Photobiology A: Chemistry*, vol. 151, no. 1-3, pp. 195–199, 2002.

[6] A. Ebrahimian, M. A. Zanjanchi, H. Noei, M. Arvand, and Y. Wang, "TiO_2 nanoparticles containing sulphonated cobalt phthalocyanine: Preparation, characterization and photocatalytic performance," *Journal of Environmental Chemical Engineering*, vol. 2, no. 1, pp. 484–494, 2014.

[7] E. Vargas, R. Vargas, and O. Núñez, "A TiO_2 surface modified with copper (II) phthalocyanine-tetrasulfonic acid tetrasodium salt as a catalyst during photoinduced dichlorvos mineralization by visible solar light," *Applied Catalysis B: Environmental*, vol. 156-157, pp. 8–14, 2014.

[8] W. A. V. Lozada, C. Diaz-Uribe, C. Quiñones, M. Lerma, C. Fajardo, and K. Navarro, "Phthalocyanines: alternative sensitizers of TiO_2 to be used in photocatalysis," *Phthalocyanines and Some Current Applications*, vol. 223, 2017.

[9] S. J. Chen, Q. Gan, H. R. Shang, and X. Liu, "Preparation and characterization of $H_3PW_{12}O_{40}/TiO_2$-M (M=Fe, Co, Ni, Zn) and photocatalytic activity for methyl orange decomposition," *Advanced Materials Research*, vol. 1073-1076, pp. 202–209, 2014.

[10] A. Pearson, S. K. Bhargava, and V. Bansal, "UV-switchable polyoxometalate sandwiched between TiO_2 and metal nanoparticles for enhanced visible and solar light photococatalysis," *Langmuir*, vol. 27, no. 15, pp. 9245–9252, 2011.

[11] H. Shi, Y. Yu, Y. Zhang et al., "Polyoxometalate/TiO_2/Ag composite nanofibers with enhanced photocatalytic performance under visible light," *Applied Catalysis B: Environmental*, vol. 221, pp. 280–289, 2018.

[12] H. Shi, T. Zhao, Y. Zhang et al., "Pt/POMs/TiO_2 composite nanofibers with an enhanced visible-light photocatalytic performance for environmental remediation," *Dalton Transactions*, vol. 48, no. 35, pp. 13353–13359, 2019.

[13] L. Li, L. Li, T. Sun et al., "Novel $H_3PW_{12}O_{40}/TiO_2$-g-C_3N_4 type-II heterojunction photocatalyst with enhanced visible-light photocatalytic properties," *Journal of Solid State Chemistry*, vol. 274, pp. 152–161, 2019.

[14] M. Taghdiri, "Selective adsorption and photocatalytic degradation of dyes using polyoxometalate hybrid supported on magnetic activated carbon nanoparticles under sunlight, visible, and UV irradiation," *International Journal of Photoenergy*, vol. 2017, Article ID 8575096, 15 pages, 2017.

[15] M. Taghdiri and S. Dadari Doolabi, "Visible/solar-light driving photocatalytic activity of TiO_2 nanotubes upon coating with phosphotungstate hybrid," *International Journal of Environmental Analytical Chemistry*, pp. 1–17, 2020.

[16] H. Mirhoseini and M. Taghdiri, "Extractive oxidation desulfurization of sulfur-containing model fuel using hexamine–phosphotungstate hybrid as effective heterogeneous catalyst," *Fuel*, vol. 167, pp. 60–67, 2016.

[17] H. Moria, T. Mohamad, and F. Aldawi, "Radiation distribution uniformization by optimized halogen lamps arrangement for a solar simulator," *Journal of Scientific and Engineering Research*, vol. 3, pp. 29–34, 2016.

[18] J. O. Jensen, "Vibrational frequencies and structural determinations of hexamethylenetetraamine," *Spectrochimica Acta Part A: Molecular and Biomolecular Spectroscopy*, vol. 58, no. 7, pp. 1347–1364, 2002.

[19] H. Yao, N. Li, S. Xu, J. Xu, J. Zhu, and H. Chen, "Electrochemical study of a new methylene blue/silicon oxide nanocomposition mediator and its application for stable biosensor of hydrogen peroxide," *Biosensors & Bioelectronics*, vol. 21, no. 2, pp. 372–377, 2005.

[20] R. Francoise and R. Jean, *Adsorption by Powders and Porous Solids; Principles*, Methodology and Applications, in, Academic Press, London, 1999.

[21] M. Pelaez, N. T. Nolan, S. C. Pillai et al., "A review on the visible light active titanium dioxide photocatalysts for environmental applications," *Applied Catalysis B: Environmental*, vol. 125, pp. 331–349, 2012.

[22] L. Ai, D. Zhang, Q. Wang, F. He, H. Yang, and Q. Wu, "Preparation of Ti-heteropolyacid/TiO_2 and its rapid photocatalytic degradation of X-3B," *Journal of Materials Science: Materials in Electronics*, vol. 31, no. 4, pp. 3166–3171, 2020.

[23] M. Moosavifar and S. Bagheri, "Photocatalytic performance of $H_6P_2W_{18}O_{62}/TiO_2$Nanocomposite encapsulated into beta zeolite under UV irradiation in the degradation of methyl orange," *Photochemistry and Photobiology*, vol. 95, no. 2, pp. 532–542, 2018.

[24] X. An, Q. Tang, H. Lan, H. Liu, and J. Qu, "Polyoxometalates/-TiO_2 Fenton-like photocatalysts with rearranged oxygen vacancies for enhanced synergetic degradation," *Applied Catalysis B: Environmental*, vol. 244, pp. 407–413, 2019.

[25] J. Zhang, W.-L. Chen, and E.-B. Wang, "Synthesis and catalytic properties of novel POM@TiO_2 composite materials," *Inorganic Chemistry Communications*, vol. 38, pp. 96–99, 2013.